Analytical Biochemistry

Volume 521, 15 March 2017, Pages 20-27

https://doi.org/10.1016/j.ab.2017.01.004

http://www.sciencedirect.com/science/article/pii/S0003269717300155

THE NOVEL TECHNIQUE OF VAPOR PRESSURE ANALYSIS TO MONITOR THE ENZYMATIC DEGRADATION OF PHB BY HPLC CHROMATOGRAPHY

Péter Polyák[1,2], Piroska Rácz[1,2], Péter Rózsa[1,2], Gergely N. Nagy[3,4], Beáta G. Vértessy[3,4], Béla Pukánszky[1,2]

[1]Laboratory of Plastics and Rubber Technology, Department of Physical Chemistry and Materials Science, Budapest University of Technology and Economics, H-1521 Budapest, P.O. Box 91, Hungary

[2]Institute of Materials and Environmental Chemistry, Research Centre for Natural Sciences, Hungarian Academy of Sciences, H-1519 Budapest, P.O. Box 286, Hungary

[3]Department of Applied Biotechnology and Food Science, Budapest University of Technology and Economics, H-1521 Budapest, P.O. Box 91, Hungary

[4]Laboratory of Genome Metabolism and Repair, Institute of Enzymology, Research Centre for Natural Sciences, Hungarian Academy of Sciences, H-1519 Budapest, P.O. Box 286, Hungary

*Corresponding author: Tel: 36-1-463-2015, Fax: 36-1-463-3474, E-mail: bpukanszky@mail.bme.hu

ABSTRACT

A novel method was introduced for the quantitative determination of substances in aqueous solutions by using the evaporative light scattering (ELS) detector of a high performance liquid chromatograph (HPLC). The principle of the measurement is the different equilibrium vapor pressure of the solvent and the analyte resulting in decreasing evaporation rate, larger droplets and stronger signal with increasing concentration. The new technique based on vapor pressure analysis was validated with traditional UV-Vis detection carried out with a diode array detector (DAD). The new technique was used for monitoring the concentration of solutions obtained during the enzymatic degradation of poly(3-hydroxybutyrate) yielding the 3-hydroxybutyrate monomer as the product. The accuracy of the measurement allowed the determination of degradation kinetics as well. The results obtained with the two techniques showed excellent agreement at small concentrations. Deviations at larger concentrations were explained with the non-linear correlation between analyte concentration and detector signal and the linear regression used for calibration. Mathematical analysis of the method made possible the determination of the evaporation enthalpy of the analyte as well. The new approach is especially suitable for the quantitative analysis of compounds, which do not absorb in the detection range of the DAD detector or if their characteristic absorbance is close to the lower end of its wavelength range.

1. INTRODUCTION

Because of its advantages, e.g. simplicity, ease of operation and convenience, UV-VIS spectrophotometry is a frequently used qualitative and quantitative analytical method in the field of biotechnology [1-5], but also in liquid chromatography [4-16]. However, besides their advantages, UV-VIS detectors have some drawbacks as well. The lack of significant UV absorbance of the analyte, or absorbance close to the lowest wavelength of the detector and the cut-off wavelength of the solvent makes determination difficult or impossible [20-21]. Other detection techniques must be applied in such cases, [17-19]. The enzymatic degradation of polyesters generally yields hydroxyl-acids [22] which absorb in the wavelength range of 190-250 nm [23,24], thus the limitations mentioned above decrease reliability. Moreover, also buffers must be often used and they absorb generally in the low UV wavelength range [23-25] and the presence of the enzyme further complicates detection, since its absorbance may influence the spectrum under 250 nm as well [26-30].

The problem of overlapping UV absorbance can be eliminated by simple baseline-correction in which the spectrum of the solution containing the buffer and the enzyme is subtracted from the spectrum of the analyte [31-34]. Castela [35] and Iwata [36], on the other hand, separated the components of the aqueous medium chromatographically and then analyzed the metabolites quantitatively. However, usually more effective detection techniques are needed to solve these problems. Refractive index detectors offer a cost effective solution [17-19], but their low sensitivity might limit the accurate determination of metabolite concentration. Destructive detection methods, like mass spectrometry [37-42], might also be used, but LC-MS-MS systems generally require rather expensive instrumentation.

In this work we propose an alternative approach to the spectroscopy-based LC detection techniques used routinely, which, unlike the vast majority of destructive LC

detectors, is cheap and quite easy to operate. The method uses a less frequently applied detection method, the evaporative light scattering detector, but in a completely new way that has not been done before. Usually the ELS detector is used for the determination of small, insoluble, solid particles. In constant nitrogen flow the dispersion is sprayed by the nebulizer into small droplets, the solvent is evaporated in a heated tube and the detector measures the light scattered on the remaining non-volatile particles. The intensity of the scattered light is proportional to the number of particles. Our method, on the other hand, does not determine solid particles, but detects the size of droplets containing the analyte and it relies on the different equilibrium vapor pressures of the components separated by the LC system.

The principle of the method is that the equilibrium vapor pressure of a solution depends on the concentration of the dissolved component, which in our case is the analyte. Instead of measuring vapor pressure, which is difficult or in our case impossible, we follow the rate of evaporation instead. A solvent (eluent) with large vapor pressure evaporates fast, but vapor pressure and thus the rate of evaporation decreases, if a component with smaller vapor pressure is dissolved in it. The solution is sprayed and moved in the heated evaporator tube, as it is usually done in ELS detection. The principle of detection is demonstrated in **Fig. 1**. The size of the dispersed droplets decreases according to their rate of evaporation, which depends on the properties and amount of the dispersed component. The droplets pass before a light source, scatter light according to their size, the intensity of which is measured by a photodetector. At larger concentration of the dissolved component, particles evaporate slower and their size remains larger at detection. The theoretical background of the method is described more in detail in the paper and calculation details are given in the Appendix.

The application of the method is demonstrated by the quantitative analysis of the metabolites produced by the enzymatic degradation of a microbial polyester, poly(3-hydroxybutyrate), PHB [43-45]. The enzyme used for catalysis originated from the strain

Bacillus Megaterium. The gene sequence, like the protein itself was discovered, isolated and characterized by Chen and his colleagues [46] who also demonstrated that the intracellular enzyme produces exclusively the monomer (3-hydroxybutyric acid) during degradation. Besides the quantitative determination of the metabolite, the approach makes possible the determination of its apparent evaporation enthalpy as well.

2. EXPERIMENTAL

2.1. Materials

Poly(3-hydroxybutyrate) granules were obtained from Metabolix Ltd. (Mirel M2100, ≥99.5% purity) with a crystallinity of ~60 %. HIS-tagged poly(3-hydroxybutyrate) depolymerase enzyme molecules were produced by recombinant *Escherichia Coli* bacteria [strain: Origami DE3 (Novagen), plasmid: pGS1865 bearing the depolymerase gene of the bacteria *Bacillus Megaterium*] and purified by affinity chromatography on a Ni-nitrilotriacedic acid (NTA) agarose column.

2.2. Sample preparation

Amorphous poly(3-hydroxybutyrate) films were prepared by compression molding and solvent casting, respectively. Films of 100 μm thickness were compression molded using a Fontijne SRA 100 machine at 120 kN, 3 min, 220 °C and at a cooling rate of about 30 °C/min. Films were cast onto a glass surface from a 2 m/m% chloroform solution of the polymer and subsequently kept at constant temperature (25 °C) and relative humidity (50 %).

2.3. Methods

The enzymatic degradation of amorphous poly(3-hydroxybutyrate) films was carried

out in Erlenmeyer flasks, at 37 °C with continuous stirring at 200 rpm. The aqueous media consisted of 100 mmol/dm^3 NaCl and 20 mmol/dm^3 tris/HCl buffer [tris(hydroxymethyl)-aminomethane hydrochloric acid salt] adjusted to pH 8.0. The amorphous polymer films and the enzyme solution were added to the Erlenmeyer flasks simultaneously, the latter in a quantity to provide 7 μg/ml enzyme concentration. The parameters (37 °C, pH 8.0 and 7 μg/ml enzyme concentration) were selected using information previously published on maximum enzyme activity [31-33].

Enzymatic degradation was monitored by recursive sampling with a time interval of 20 min, over a 3 hour period. The samples were analyzed using a reversed phase liquid chromatograph (Merck-Hitachni LaChrom Elite) equipped with a LiChroChart 250-4 column. The column contained LiChrospher 100 RP-18 type end-capped silica with an average particle diameter of 5 μm and pore size of 100 nm.

The reversed phase LC system was equipped with a Polymer Laboratories PL-ELS2100 Ice detector, which was used as indirect vapor pressure analyzer over the temperature range of 35-50 °C. As sufficient detector sensitivity requires the equilibrium vapor pressure of the eluent and the analyte to be significantly different, the pH of the eluent was regulated with a volatile acid/salt buffer (HCOOH/NH_4COOH) with the concentration of 10 mmol/dm^3 at pH 3.0.

Reference measurements were carried out with the diode array detector of the LaChrom Elite liquid chromatograph. As the UV absorbance of the volatile buffer used for vapor pressure analysis (HCOOH/NH_4COOH) overlaps with the absorbance peak of the metabolite (3-hydroxybutyric acid), adequate quantitative measurement based on UV absorbance required a buffer which did not absorb in the UV range. The buffer must also have provided stable pH at 3.0, which was achieved with the H_3PO_4/KH_2PO_4 phosphate buffer at the same, 10 mmol/dm^3 concentration. The DAD detector measured the 190-300

nm range with the time interval of 400 ms. Eluent flow was kept constant at 1.0 ml/min both in the measurements based on vapor pressure analysis and on UV detection.

3. RESULTS

3.1. Vapor pressure analysis

According to Raoult's law, increasing concentration of a liquid phase component with smaller equilibrium vapor pressure results in decreasing pressure of the vapor above the solution. As the equilibrium vapor pressure of each component of the aqueous media analyzed (tris buffer, NaCl, enzyme and the monomer) is significantly smaller than that of the eluent (10 mmol/dm^3 HCOOH/NH_4COOH buffer), the pressure of the vapor phase is smaller, when it contains any of the analytes listed above. When the eluent-analyte solution is evaporated, smaller equilibrium vapor pressure results in slower phase transition and thus slower evaporation rate.

A detection technique based on vapor pressure analysis requires a nebulizer dispersing the eluent flow into liquid droplets carried by an inert gas flow, which is usually dry nitrogen or argon. The evaporation of a droplet begins immediately when it leaves the nebulizer and enters the evaporator tube, which is equipped with a photodetector at the other end. If the eluent carries an analyte with smaller equilibrium pressure, the evaporation of the droplet slows down resulting in larger particles. The detector determines particle size by measuring scattered light, i.e. droplets with larger average diameter scatter more photons resulting in stronger detector signal. Chromatograms recorded by the ELS detector on solutions obtained after different times of enzymatic degradation are plotted in **Fig. 2**.

The first peak appears at 2 min and its intensity is independent of the time of degradation. It belongs to the ionized components of the aqueous media (NaCl salt, tris buffer and enzyme molecules), as these ions are barely detained by the RP-18 endcapped

silica column, and thus their retention time is close to the t_0 value of the column (~1.90-1.95 min). Due to the practically zero equilibrium vapor pressure of the components listed above, the decrease of the evaporation rate results in the formation of droplets with a diameter outside the range of the detector. The constant height and shape of this peak indicates that the concentration of the ionized components (NaCl salt, tris buffer and enzyme molecules) remains constant throughout the entire time interval measured.

The height of the peak eluting at 6 minutes, however, depends significantly on time because of the formation of 3-hydroxybutyric acid during enzymatic degradation (**Fig. 3**). While the charge of the buffer components applied to set the pH of the aqueous media (Na^+, Cl^- and tris ions) is not affected by the acidity of the eluent, the monomer with a pKa value of 4.70 can be protonated at pH 3.0. The dipole moment of a protonated acid molecule is generally significantly smaller than that of the deprotonated ion, which increases its retention time. Increased retention time (about 6 minutes, see **Figs. 2** and 3) provides excellent separation efficiency and makes possible the quantitative determination of the concentration of the monomer separated from the other components by the column.

Because the presence of the buffer (10 mmol/dm^3 $HCOOH/NH_4COOH$) shifts the signal measured for the pure eluent to 140 mV (see **Figs. 1** and **2**) base line correction is needed and the integration of the peaks results in a quantity proportional to the concentration of the analyte. Quantitative analysis allows the determination of degradation kinetics. As **Fig. 4** demonstrates, the enzyme starts to react with an initial accelerating stage, but reaction rate eventually reaches a constant value, which prevails until the end of the measurement. Although the results obtained by vapor pressure analysis seem to be reasonable and the kinetics of degradation corresponds to expectations, the new method must be validated with an accepted technique, e.g. by UV-Vis detection.

3.2. UV detection

Although the DAD was set to measure the entire wavelength range (190-300 nm), only absorbances recorded at 215 nm, at the maximum absorbance of the monomer molecules, were used in the quantitative analysis. The comparison of **Figs. 2** and 5 demonstrates the most important difference between the two detection techniques used, i.e. vapor pressure analysis and UV spectroscopy. Compared to the absorbance of the monomer, the first peak with a retention time of approximately 2 minutes is significantly smaller in **Fig. 5** than the one recorded with the ELS detector (see **Fig. 2**). The NaCl concentration of the analyzed aqueous media was relatively large (0.1 mol/dm^3), yet the equilibrium vapor pressure of this component is practically zero. This causes the eluent-NaCl solution to evaporate slowly resulting in the formation of relatively large droplets leading to a strong signal in ELS detection. Accordingly, the signal detected in the vapor pressure analysis is especially sensitive to the presence of non-volatile components. However, the DAD detector (see **Fig. 5**) gave a considerably smaller signal in this range, since the UV absorbance of Na^+ and Cl^- ions is practically zero in the entire 190-300 nm wavelength range. The relatively weak signal detected at around 2 min can be attributed to the absorption of the tris/HCL buffer and the enzyme molecules, but the concentration of these latter is much smaller than that of the buffer.

On the other hand, the peaks attributed to the protonated monomer detected by the two techniques are quite similar independently of the detection technique used. This similarity originates from the physical characteristics of the monomer (3-hydroxybutyric acid) molecules. The electrons of the carboxyl group present in the molecule result in significant UV absorbance, on the one hand, while 3-hydroxybutyric acid has a relatively low equilibrium vapor pressure, on the other, which makes it ideal as a reference material for the comparison of the two techniques.

Similarly to the vapor pressure analysis, the kinetics of enzymatic degradation was determined also with UV detection. The results obtained are presented in **Fig. 6**. The similarity of the correlations to those shown in **Fig. 4** is striking indicating that the two detection techniques yield very similar data at least qualitatively. A more detailed analysis is needed to check the agreement quantitatively.

3.3. Comparison

The direct comparison of the results requires the preliminary calibration of the detectors with an internal standard. 3-hydroxybutyric acid with >95% purity is available as a commercial product. Using this product allows the determination of the calibration parameters required to convert detector signals into concentrations. The concentrations determined in the calibrating solutions are plotted against each other in **Fig. 7.**

The comparison of the results obtained with the two detection techniques reveals that at small concentrations the vapor pressure analysis based detection technique is just as reliable as the other method used for validation (UV). However, at larger concentrations the UV detection provides considerably larger values indicating that the measurement based on vapor pressure analysis is biased by a concentration dependent systematic error (see **Fig. 7**). This error is caused by the nonlinear correlation between analyte concentration and detector signal and by the fact that calibration constants were calculated with a simple linear regression for both detectors. One either eliminates this anomaly with the application of a nonlinear calibration curve, or continues to use linear regression and applies the calibration only at low analyte concentrations.

3.4. Temperature dependence

The results presented above unambiguously proved that the novel chromatographic

detection method based on vapor pressure analysis is an excellent tool for the study of the enzymatic degradation of microbial polyesters. Measurements carried out as a function of temperature yield further information about the compound analyzed. The equilibrium vapor pressure of the eluent changes with changing temperature of the evaporator tube resulting in a modification of evaporation rate. Changes in equilibrium vapor pressure over an aqueous phase as a function of temperature can be estimated by the Clausius-Clapeyron equation which contains the apparent evaporation enthalpy of the compound in question. Measurements carried out as a function of temperature allow the determination of this quantity which is characteristic for the analyte studied.

In order to check the validity of the principle, chromatograms were recorded in the temperature range of 35-50 °C. As the ionized components (NaCl salt and tris/HCl buffer) are non-volatile, the peak eluted at 2 minutes does not depend on temperature. On the other hand, the height of the second peak attributed to protonated 3-hydroxybutyric acid molecules was drastically modified by changing temperature. At 36 °C the signal of the monomer is significant, but at 50 °C it is close to the detection limit (see **Fig. 7**). The considerable temperature dependence of the detected peak allows us the determination of evaporation enthalpy, but to achieve this further considerations and calculations are needed.

4. DISCUSSION

The Clausius-Clapeyron equation forming the basis of our approach takes the following form

$$\ln\frac{p_1}{p_2}=\frac{\Delta H}{R}\left(\frac{1}{T_1}-\frac{1}{T_2}\right) \qquad (1)$$

where p_1 and T_1 are the equilibrium vapor pressure and temperature, respectively, in state 1, while p_2 and T_2 are the same quantities in state 2. State 1 is generally the state being

investigated, while state 2 is a reference state, most frequently the standard state. ΔH is the apparent evaporation enthalpy of the material in question while R the universal gas constant.

In our case, however, the vapor pressure of the state being measured is required as a direct function of temperature. The rearrangement of **Eq. 1** and the merging of constants results in the required function

$$p_1 = C \exp\left(-\frac{\Delta H}{R\,T}\right) \tag{2}$$

Eq. 2 describes the temperature dependence of vapor pressure, but the detector supplies a signal related to droplet size and not directly the vapor pressure of the eluent. The calculation of droplet size requires the knowledge of the rate of evaporation, which depends on the equilibrium vapor pressure of the eluent (**Eq. 2**). For the sake of simplicity, this positive correlation is approximated with a linear function

$$v_e = k_e\ p_1 \tag{3}$$

where v_e is the rate of the evaporation, k_e is a constant and p_1 is the equilibrium vapor pressure of the eluent. The latter is the driving force of evaporation, since at the moment of the droplet formation the vapor pressure of the eluent is zero in the dry nitrogen flow. By merging **Eqs. 2 and 3** one obtains

$$v_e(T) = k_e\, C \exp\left(-\frac{\Delta H}{R\,T}\right) \tag{4}$$

which gives the temperature dependence of evaporation rate directly. The average size of the droplets reaching the end of the evaporator tube can also be estimated from **Eq. 4**. The droplets are analyzed by a photodetector, which generates a signal related to the ratio of emitted photons to scattered photons. Such a relationship can be described by a number of models used for the description of photon scattering.

In our treatment we use the Rayleigh scattering. The application of the approach in

our specific case is described in the **Appendix**. The function derived relates the intensity of detector signal to temperature and allows the estimation of peak areas as a function of temperature (see **Fig. 8**)

$$U_d = A_i\left[r_{\max} - C'\exp\left(-\frac{\Delta H}{R\,T}\right)\right] \qquad (5)$$

where U_d is the output voltage of the detector (millivolts) A_i is an instrument specific constant (mV/nm), $r_{\max}$ is the average diameter of the droplets at the beginning of their evaporation (nm) and C' is a pre-exponential coefficient containing the constants of the standard state as well as the rate constant of evaporation (nm). Since the function presented in **Eq. 5** is not linear and it cannot be linearized either, the fitting of **Eq. 5** onto the experimental data requires a nonlinear, iterative algorithm, which was the Levenberg-Marquardt algorithm in our case. The result of the fitting procedure is shown in **Fig. 9**.

Fig. 9 shows very good agreement between the measured values and the fitted correlation. The fitting procedure yielded also the numerical values of the constants including the enthalpy of evaporation. Considering the technical difficulties of the measurement and the computational procedure, the value obtained by us (82.5 kJ/mol) agrees reasonably well with published values (67.5 kJ/mol) [47,48]. The deviation between the two values can be explained with the different temperature range of the actual measurements (308-323 K in our case, 371-485 K published), on the one hand, and with the uncertainty of the determination of droplet size.

5. CONCLUSIONS

A novel method was introduced for the quantitative determination of substances in aqueous solutions by using the ELS detector of a HPLC chromatograph. The principle of the measurement is the different equilibrium vapor pressure of the solvent and the analyte

resulting in decreasing evaporation rate, larger droplets and stronger signal with increasing concentration. The new technique based on vapor pressure analysis was validated with traditional UV-Vis detection carried out with a diode array detector. The new technique was used for monitoring the concentration of solutions obtained during the enzymatic degradation of poly(3-hydroxybutyrate) yielding the 3-hydroxybutyrate monomer as the product. The accuracy of the measurement allowed the determination of degradation kinetics as well. The results obtained with the two techniques showed excellent agreement at small concentrations. Deviations at larger concentrations were explained with the non-linear correlation between analyte concentration and detector signal and the linear regression used for calibration. Mathematical analysis of the method made possible the determination of the evaporation enthalpy of the analyte. The new approach is especially suitable for the quantitative analysis of compounds, which do not absorb in the detection range of the DAD detector or if their characteristic absorbance is close to the lower end of its wavelength range.

ACKNOWLEDGEMENTS

The authors are indebted to László Cseke for his help in the development of the LC detection method based on vapor pressure analysis, to Ramóna Bende for her assistance in sample preparation and to Ildikó Erdőné Fazekas for her valuable contribution to the HPLC measurements. The National Research Fund of Hungary (OTKA K 120039, OTKA K 109486 and ICGEB CRP/HUN 14-01) is greatly acknowledged for the financial support of the research.

REFERENCES

[1] R. Lange, C. Balny, UV-visible derivative spectroscopy under high pressure, Biochimica Et Biophysica Acta-Protein Structure and Molecular Enzymology, 1595

(2002) 80-93.

[2] M. Sirajuddin, S. Ali, A. Badshah, Drug-DNA interactions and their study by UV-Visible, fluorescence spectroscopies and cyclic voltametry, Journal of Photochemistry and Photobiology B-Biology, 124 (2013) 1-19.

[3] M. Samsonowicz, I. Kaminska, M. Kalinowska, W. Lewandowski, Alkali metal salts of rutin - Synthesis, spectroscopic (FT-IR, FT-Raman, UV-VIS), antioxidant and antimicrobial studies, Spectrochimica Acta Part a-Molecular and Biomolecular Spectroscopy, 151 (2015) 926-938.

[4] J.Q. Brown, K. Vishwanath, G.M. Palmer, N. Ramanujam, Advances in quantitative UV-visible spectroscopy for clinical and pre-clinical application in cancer, Current Opinion in Biotechnology, 20 (2009) 119-131.

[5] F. Pena-Pereira, I. Costas-Mora, V. Romero, I. Lavilla, C. Bendicho, Advances in miniaturized UV-Vis spectrometric systems, Trac-Trends in Analytical Chemistry, 30 (2011) 1637-1648.

[6] C.J. Peer, T.J. McManus, H.I. Hurwitz, W.P. Petros, Development and utilization of a combined LC-UV and LC-MS/MS method for the simultaneous analysis of tegafur and 5-fluorouracil in human plasma to support a phase I clinical study of oral UFT (R)/leucovorin, Journal of Chromatography B-Analytical Technologies in the Biomedical and Life Sciences, 898 (2012) 32-37.

[7] A.A. Almousa, R. Ikeda, M. Wada, N. Kuroda, R.-K. Hanajiri, K. Nakashima, HPLC-UV method development for fentanyl determination in rat plasma and its application to elucidate pharmacokinetic behavior after i.p. administration to rats, Journal of Chromatography B-Analytical Technologies in the Biomedical and Life Sciences, 879 (2011) 2941-2944.

[8] S.D. Chitnis, F. Akhlaghi, Development and validation of an HPLC-UV method for

iodixanol quantification in human plasma, Journal of Chromatography B-Analytical Technologies in the Biomedical and Life Sciences, 869 (2008) 133-137.

[9] A. Loregian, M.C. Scarpa, S. Pagni, S.G. Parisi, G. Palu, Measurement of ribavirin and evaluation of its stability in human plasma by high-performance liquid chromatography with UV detection, Journal of Chromatography B-Analytical Technologies in the Biomedical and Life Sciences, 856 (2007) 358-364.

[10] N. Rastkari, M. Khoobi, A. Shafiee, M.R. Khoshayand, R. Ahmadkhaniha, Development and validation of a simple and sensitive HPLC-UV method for the determination of captopril in human plasma using a new derivatizing reagent 2-naphthyl propiolate, Journal of Chromatography B-Analytical Technologies in the Biomedical and Life Sciences, 932 (2013) 144-151.

[11] E. Giraud, E. Rey, J.M. Treluyer, G. Pons, V. Jullien, Quantification of tipranavir in human plasma by high-performance liquid chromatography with UV detection, Journal of Chromatography B-Analytical Technologies in the Biomedical and Life Sciences, 830 (2006) 86-90.

[12] K. Safranow, Z. Machoy, Simultaneous determination of 16 purine derivatives in urinary calculi by gradient reversed-phase high-performance liquid chromatography with UV detection, Journal of Chromatography B-Analytical Technologies in the Biomedical and Life Sciences, 819 (2005) 229-235.

[13] R. Mirzajani, F. Kardani, Fabrication of ciprofloxacin molecular imprinted polymer coating on a stainless steel wire as a selective solid-phase microextraction fiber for sensitive determination of fluoroquinolones in biological fluids and tablet formulation using HPLC-UV detection, Journal of Pharmaceutical and Biomedical Analysis, 122 (2016) 98-109.

[14] A. Khan, Z. Iqbal, I. Khadra, L. Ahmad, A. Khan, M.I. Khan, Z.I. Ullah, Simultaneous

determination of domperidone and Itopride in pharmaceuticals and human plasma using RP-HPLC/UV detection: Method development, validation and application of the method in in-vivo evaluation of fast dispersible tablets, Journal of Pharmaceutical and Biomedical Analysis, 121 (2016) 6-12.

[15] M. Al-Sibani, A. Al-Harrasi, R.H.H. Neubert, Evaluation of in-vitro degradation rate of hyaluronic acid-based hydrogel cross-linked with 1, 4-butanediol diglycidyl ether (BDDE) using RP-HPLC and UV-Vis spectroscopy, Journal of Drug Delivery Science and Technology, 29 (2015) 24-30.

[16] M. Miura, N. Takahashi, Routine therapeutic drug monitoring of tyrosine kinase inhibitors by HPLC-UV or LC-MS/MS methods, Drug Metabolism and Pharmacokinetics, 31 (2016) 12-20.

[17] A. Peepliwal, C.G. Bonde, K.G. Bothara, A validated RP-HPLC method for quantitative determination of related impurities of ursodeoxycholic acid (API) by refractive index detection, Journal of Pharmaceutical and Biomedical Analysis, 54 (2011) 845-849.

[18] D. Brennan, P. O'Brien, J. O'Brien, N. Freeman, M. Swann, Development and test of an integrated microsystem for HPLC separation and detection using refractive index measurements, Sensors and Actuators B-Chemical, 103 (2004) 184-189.

[19] A.D. McBrady, R.E. Synovec, Microfabricated refractive index gradient based detector for reversed-phase liquid chromatography with mobile phase gradient elution, Journal of Chromatography A, 1105 (2006) 2-10.

[20] F.M. Miroiu, N. Stefan, A.I. Visan, C. Nita, C.R. Luculescu, O. Rasoga, M. Socol, I. Zgura, R. Cristescu, D. Craciun, G. Socol, Composite biodegradable biopolymer coatings of silk fibroin - Poly(3-hydroxybutyric-acid-co-3-hydroxyvaleric-acid) for biomedical applications, Applied Surface Science, 355 (2015) 1123-1131.

[21] J. He, S.W. Chen, Z.N. Yu, Determination of poly-beta-hydroxybutyric acid in Bacillus thuringiensis by capillary zone electrophoresis with indirect ultraviolet absorbance detection, Journal of Chromatography A, 973 (2002) 197-202.

[22] C.W. Pouton, S. Akhtar, Biosynthetic polyhydroxyalkanoates and their potential in drug delivery, Advanced Drug Delivery Reviews, 18 (1996) 133-162.

[23] R. Vespalec, M. Vlckova, H. Horakova, Aggregation and other intermolecular interactions of biological buffers observed by capillary electrophoresis and UV photometry, Journal of Chromatography A, 1051 (2004) 75-84.

[24] A. Luis, T.B.V. Dinis, H. Passos, M. Taha, M.G. Freire, Good's buffers as novel phase-forming components of ionic-liquid-based aqueous biphasic systems, Biochemical Engineering Journal, 101 (2015) 142-149.

[25] M. Taha, M.V. Quental, I. Correia, M.G. Freire, J.A.P. Coutinho, Extraction and stability of bovine serum albumin (BSA) using cholinium-based Good's buffers ionic liquids, Process Biochemistry, 50 (2015) 1158-1166.

[26] L. Li, Y. Shen, Y.-H. Zhao, L. Mu, X. Zeng, C. Redshaw, G. Wei, A single chemosensor for multiple analytes: Fluorogenic and ratiometric absorbance detection of Zn2+, Mg2+ and F-, and its cell imaging, Sensors and Actuators B-Chemical, 226 (2016) 279-288.

[27] A. Suthaparan, K.A. Solhaug, A. Stensvand, H.R. Gislerod, Determination of UV action spectra affecting the infection process of Oidium neolycopersici, the cause of tomato powdery mildew, Journal of Photochemistry and Photobiology B-Biology, 156 (2016) 41-49.

[28] A. Kumar, A.K. Srivastava, S. Gangwar, N. Misra, A. Mondal, G. Brahmachari, Combined experimental (FT-IR, UV-visible spectra, NMR) and theoretical studies on the molecular structure, vibrational spectra, HOMO, LUMO, MESP surfaces,

reactivity descriptor and molecular docking of Phomarin, Journal of Molecular Structure, 1096 (2015) 94-101.

[29] D. Singh, R.M. Schaaper, A. Hochkoeppler, A continuous spectrophotometric enzyme-coupled assay for deoxynucleoside triphosphate triphosphohydrolases, Analytical Biochemistry, 496 (2016) 43-49.

[30] K. Musil, V. Florianova, P. Bucek, V. Dohnal, K. Kuca, K. Musilek, Development and validation of a FIA/UV-vis method for pK(a) determination of oxime based acetylcholinesterase reactivators, Journal of Pharmaceutical and Biomedical Analysis, 117 (2016) 240-246.

[31] K. Kasuya, Y. Doi, T. Yao, Enzymatic degradation of poly (r)-3-hydroxybutyrate by comamonas testosteroni-atsu of soil bacterium, Polymer Degradation and Stability, 45 (1994) 379-386.

[32] K. Kasuya, Y. Inoue, K. Yamada, Y. Doi, Kinetics of surface hydrolysis of poly (r)3-hydroxybutyrate film by phb depolymerase from alcaligenes-faecalis t1, Polymer Degradation and Stability, 48 (1995) 167-174.

[33] K. Mukai, K. Yamada, Y. Doi, Kinetics and mechanism of heterogeneous hydrolysis of poly (r)-3-hydroxybutyrate film by pha depolymerases, International Journal of Biological Macromolecules, 15 (1993) 361-366.

[34] M. Scandola, M.L. Focarete, G. Frisoni, Simple kinetic model for the heterogeneous enzymatic hydrolysis of natural poly(3-hydroxybutyrate), Macromolecules, 31 (1998) 3846-3851.

[35] J. Mascastella, J. Urmeneta, R. Lafuente, A. Navarrete, R. Guerrero, Biodegradation of poly-beta-hydroxyalkanoates in anaerobic sediments, International Biodeterioration & Biodegradation, 35 (1995) 155-174.

[36] T. Iwata, Y. Doi, S. Nakayama, H. Sasatsuki, S. Teramachi, Structure and enzymatic

degradation of poly(3-hydroxybutyrate) copolymer single crystals with an extracellular PHB depolymerase from Alcaligenes faecalis T1, International Journal of Biological Macromolecules, 25 (1999) 169-176.

[37] G. Adamus, W. Sikorska, H. Janeczek, M. Kwiecien, M. Sobota, M. Kowalczuk, Novel block copolymers of atactic PHB with natural PHA for cardiovascular engineering: Synthesis and characterization, European Polymer Journal, 48 (2012) 621-631.

[38] M.P. Arrieta, J. Lopez, E. Rayon, A. Jimenez, Disintegrability under composting conditions of plasticized PLA-PHB blends, Polymer Degradation and Stability, 108 (2014) 307-318.

[39] M.P. Arrieta, E. Fortunati, F. Dominici, E. Rayon, J. Lopez, J.M. Kenny, PLA-PHB/cellulose based films: Mechanical, barrier and disintegration properties, Polymer Degradation and Stability, 107 (2014) 139-149.

[40] P. Rizzarelli, S. Carroccio, Modern mass spectrometry in the characterization and degradation of biodegradable polymers, Analytica Chimica Acta, 808 (2014) 18-43.

[41] M. Maksymiak, M. Kowalczuk, G. Adamus, Electrospray tandem mass spectrometry for the structural characterization of p-coumaric acid-oligo (3-hydroxybutyrate) conjugates, International Journal of Mass Spectrometry, 359 (2014) 6-11.

[42] R. Goodacre, D.B. Kell, Pyrolysis mass spectrometry and its applications in biotechnology, Current Opinion in Biotechnology, 7 (1996) 20-28.

[43] P. Suriyamongkol, R. Weselake, S. Narine, M. Moloney, S. Shah, Biotechnological approaches for the production of polyhydroxyalkanoates in microorganisms and plants – A review, Biotechnology Advances, 25 (2007) 148-175.

[44] Y. Wang, J. Yin, G.-Q. Chen, Polyhydroxyalkanoates, challenges and opportunities, Current Opinion in Biotechnology, 30 (2014) 59-65.

[45] R. Li, H. Zhang, Q. Qi, The production of polyhydroxyalkanoates in recombinant Escherichia coli, Bioresource Technology, 98 (2007) 2313-2320.

[46] H.J. Chen, S.C. Pan, G.C. Shaw, Identification and Characterization of a Novel Intracellular Poly(3-Hydroxybutyrate) Depolymerase from Bacillus megaterium, Applied and Environmental Microbiology, 75 (2009) 5290-5299.

[47] J.S. Chickos, W.E. Acree, Enthalpies of vaporization of organic and organometallic compounds, 1880-2002, Journal of Physical and Chemical Reference Data, 32 (2003) 519-878.

[48] R.M. Stephenson, S. Malanowski, Handbook of the Thermodynamics of Organic Compounds, Elsevier, New York, 1987.

APPENDIX

According to the Rayleigh theory, the amount of scattered photons can be calculated as

$$I = I_0 \frac{1+\cos^2\theta}{2R^2}\left(\frac{2\pi}{\lambda}\right)^4\left(\frac{n^2-1}{n^2+2}\right)^2\left(\frac{d}{2}\right)^6 \quad (1)$$

where I_0 is the intensity of the photon source, θ the scattering angle, R the distance of the photon source to the particle, λ the wavelength of the photons scattered, n the refractive index and d is the diameter of the particle.

The rate of evaporation in the ELS detector is proportional to the surface of the particles and depends on time (t). Accordingly the rate of evaporation can be expressed as

$$v_e(t) = \frac{\mathrm{d}V(t)}{\mathrm{d}t} = -k\,4\pi\,r(t)^2 \quad (2)$$

where V is the volume and r the radius of the droplets. Volume can be expressed in terms of radius, thus evaporation rate takes the form

$$v_e(t) = -k'\left[\frac{4}{3}\pi\,r(t)^3\right]^{\frac{2}{3}} \quad (3)$$

where k' is a constant. Expressing the right hand side of the equation in volume again leads to the homogeneous first order differential equation

$$\frac{dV(t)}{dt} = -k'V(t)^{\frac{2}{3}} \quad (4)$$

Separation of the variables and integration gives us the time dependent volume of the droplets

$$V(t) = \left(-\frac{k'}{3}t + c\right)^3 \quad (5)$$

However, the intensity of scattering depends on the size of the particles and not on their volume, thus we must express **Eq. A5** in terms of size in order to obtain time dependent particle size

$$r(t)=\left(\frac{3}{4\pi}\right)^{\frac{1}{3}}\left(-\frac{k'}{3}t+c\right) \tag{6}$$

Eq. A6 shows that particle size depends linearly on the time of flight.

The size of droplets depends on temperature and on their position in the evaporator tube. The final size of the droplet (r_r) can be calculated from its initial size (r_{max}), particle size decreases continuously and linearly as it passes along the tube. Accordingly

$$r_r = r_{max} - C' \exp\left(\frac{\Delta H}{R\,T}\right) \tag{7}$$

where *C*' contains all constants related to the reference state and the geometry of the evaporation tube. Introducing **Eq. A7** into Rayleigh's equation (**Eq. A1**), yields the final correlation for temperature dependent detector intensity

$$U_d = A_i\left[r_{max} - C' \exp\left(\frac{\Delta H}{R\,T}\right)\right]^6 \tag{8}$$

CAPTIONS

Fig. 1 Schematic drawing of the detection system of used in the vapor pressure approach.

Fig. 2 Dependence of the intensity of the signal detected by vapor pressure analysis (ELS detector) on aqueous solutions obtained by the enzymatic degradation of PHB as a function of time. Sample: compression molded film, temperature: 36 °C. Degradation time increases from 0 to 180 min.

Fig. 3 Increasing height of the peak assigned to the degradation product, 3-hydroxybutirate. Conditions are the same as in **Fig. 2**.

Fig. 4 Kinetics of the enzymatic degradation of PHB determined by vapor pressure analysis. Symbols: (□) compression molding, (△) solvent casting. Other conditions are the same as in **Fig. 2**.

Fig. 5 Chromatograms recorded on degradation solutions by UV detection at 215 nm as a function of degradation time. Sample: compression molded film.

Fig. 6 Kinetics of the enzymatic degradation of PHB determined by the UV detection of the concentration of the resulting monomer. Symbols: (□) compression molding, (△) solvent casting.

Fig. 7 Comparison of monomer concentrations determined by traditional UV detection and vapor pressure analysis (ELS detector).

Fig. 8 Temperature dependence of the signal recorded by the ELS detector (vapor pressure analysis) on aqueous solutions containing the 3-hydroxybutyrate monomer after 180 min enzymatic degradation of a compression molded PHB film.

Fig. 9 Effect of temperature on the intensity of the signal recorded by vapor pressure analysis (ELS detector). Degradation time: 180 min, sample: compression

molded film. Symbols: (□) measured data, ——— fitted correlation.

FIGURES

Polyák, Fig. 1

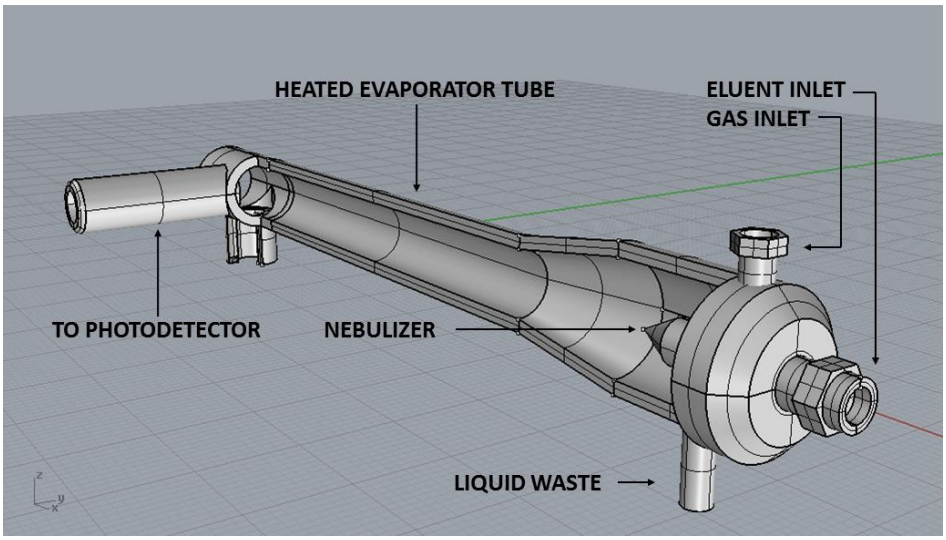

Polyák, Fig. 2

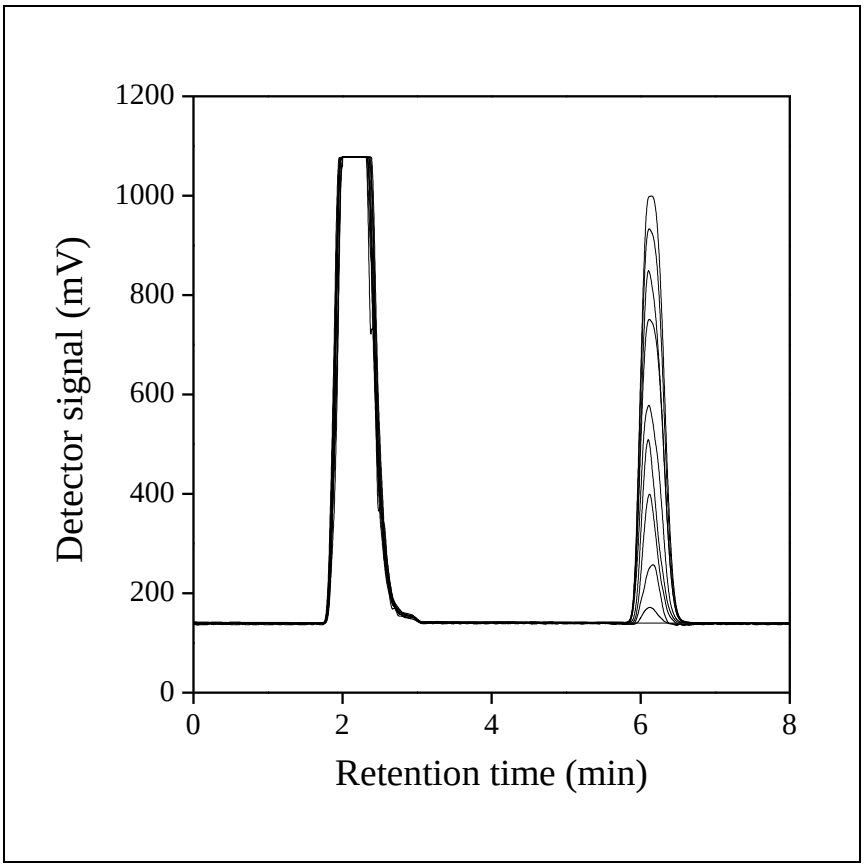
Detector signal (mV)
1200
1000
800
600
400
200
0
0
2
4
6
8
Retention time (min)

Polyák, Fig. 3

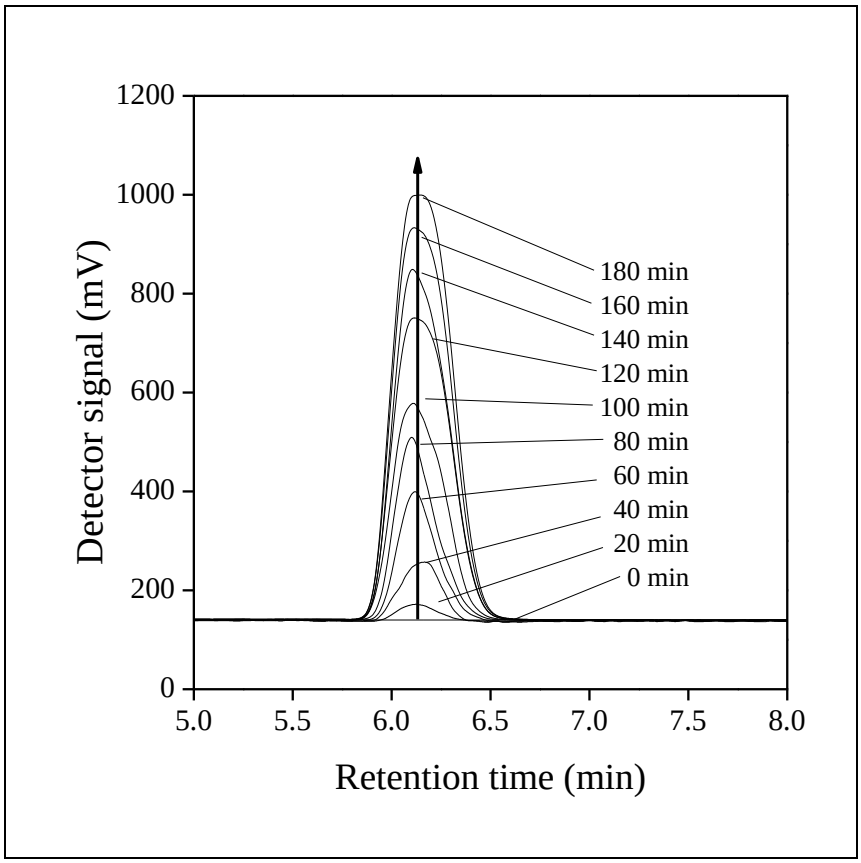
Detector signal (mV)
Retention time (min)
0
200
400
600
800
1000
1200
5.0
5.5
6.0
6.5
7.0
7.5
8.0
180 min
160 min
140 min
120 min
100 min
80 min
60 min
40 min
20 min
0 min

Polyák, Fig. 4

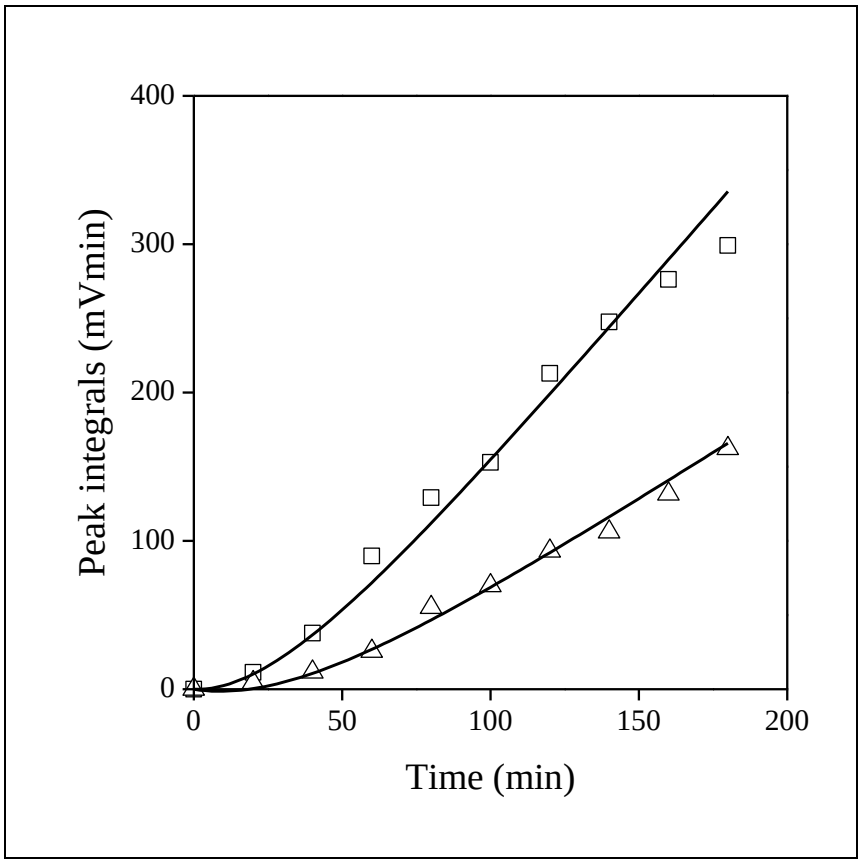
400
300
200
100
0
Peak integrals (mVmin)
0
50
100
150
200
Time (min)

Polyák, Fig. 5

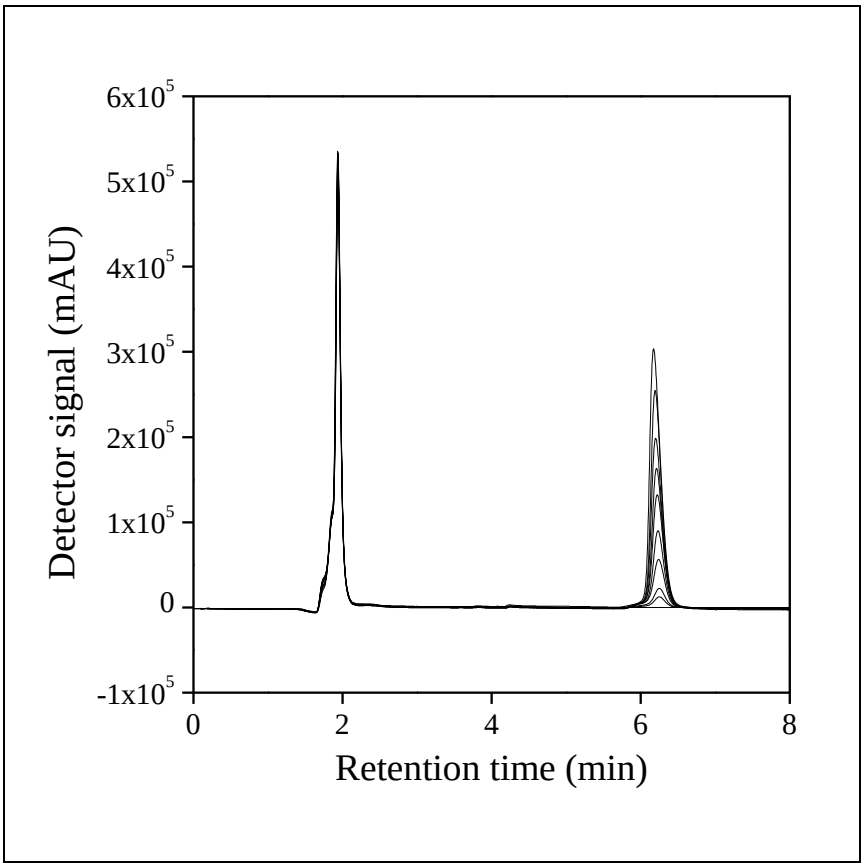
6x10^5
5x10^5
4x10^5
3x10^5
2x10^5
1x10^5
0
-1x10^5
Detector signal (mAU)
0
2
4
6
8
Retention time (min)

Polyák, Fig. 6

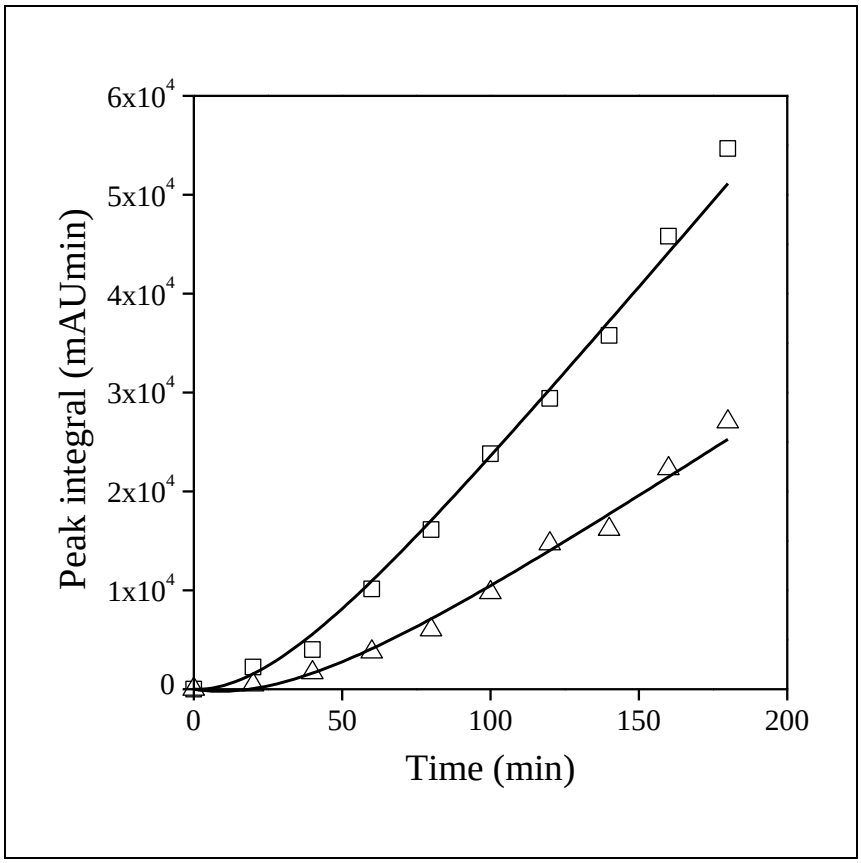
Peak integral (mAUmin)
6x10^4
5x10^4
4x10^4
3x10^4
2x10^4
1x10^4
0
0
50
100
150
200
Time (min)

Polyák, Fig. 7

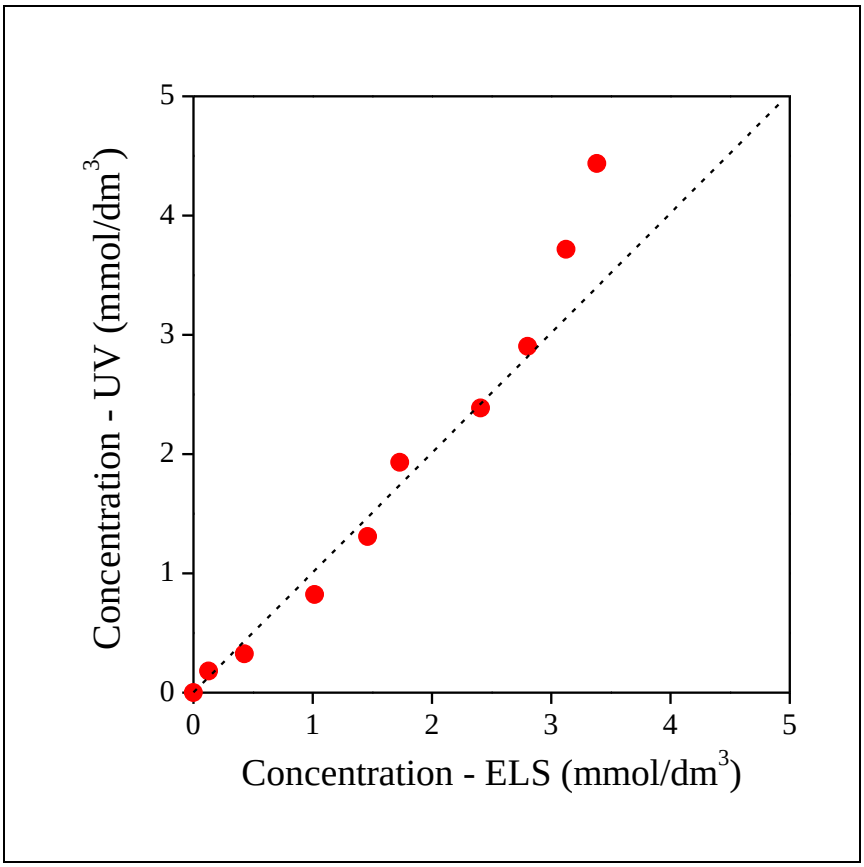
Concentration - UV (mmol/dm3)
Concentration - ELS (mmol/dm3)
0
1
2
3
4
5

Polyák, Fig. 8

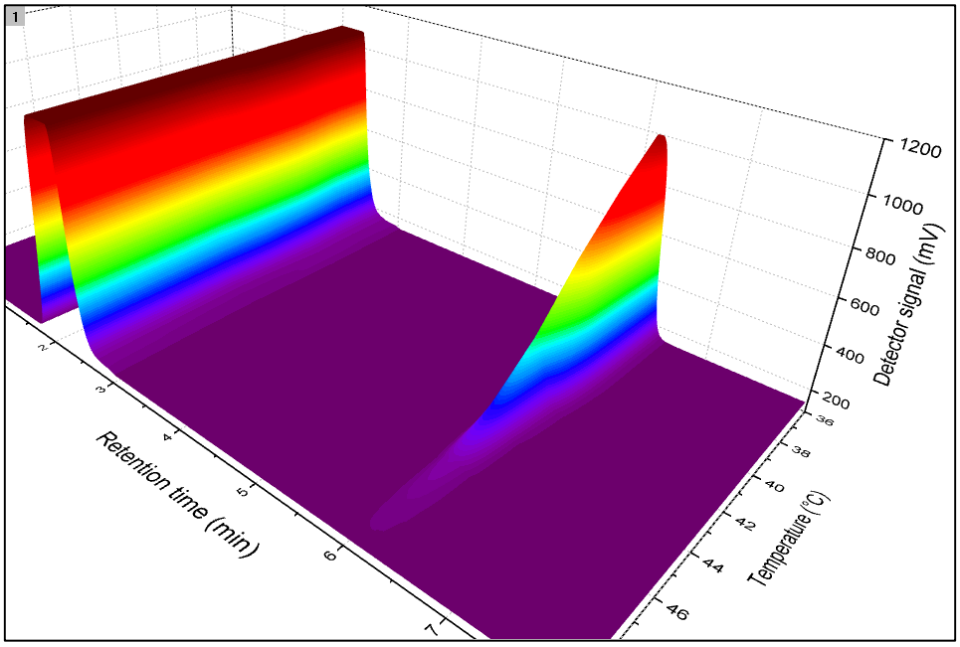
1
Retention time (min)
Temperature (°C)
Detector signal (mV)
1200
1000
800
600
400
200

Polyák, Fig. 9

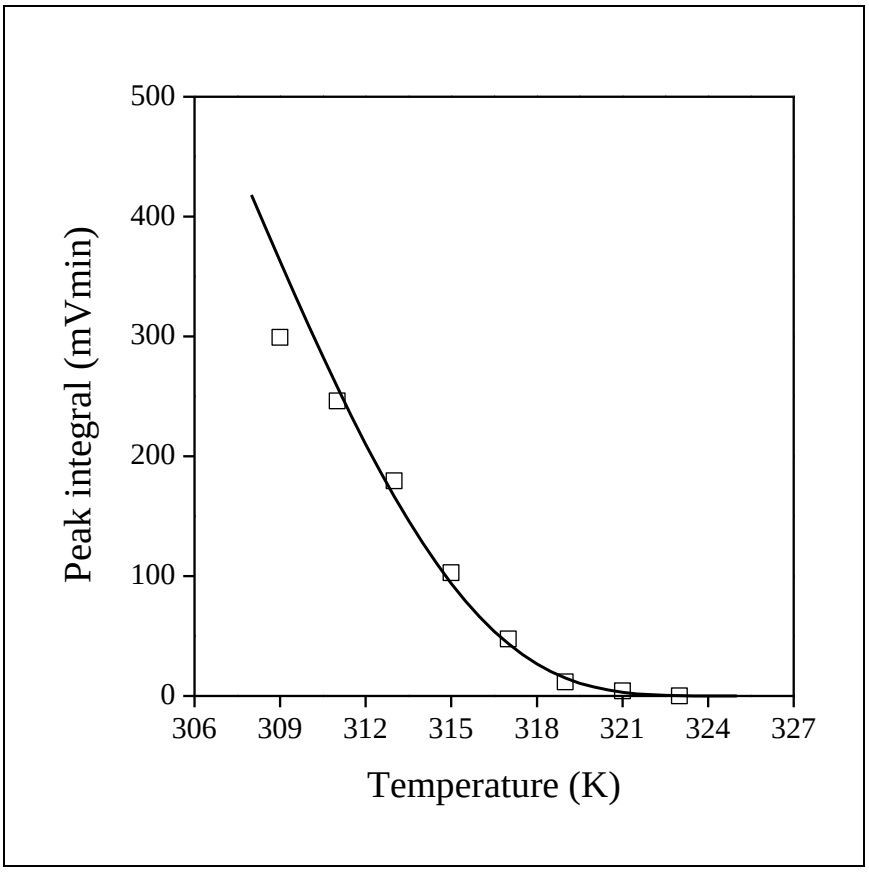
500
400
300
200
100
0
Peak integral (mVmin)
306
309
312
315
318
321
324
327
Temperature (K)